Catalysis Today 228 (2014) 167–174

Contents lists available at ScienceDirect

Catalysis Today

journal homepage: www.elsevier.com/locate/cattod

Selective synthesis of gasoline from syngas in near-critical phase

Ting Ma[a], Hiroyuki Imai[a,*], Yoshifumi Suehiro[b], Chun Chen[a], Toshiyuki Kimura[a], Sachio Asaoka[a], Xiaohong Li[a]

[a] *Faculty of Environmental Engineering, The University of Kitakyushu, 1-1 Hibikino, Wakamatsu, Kitakyushu, Fukuoka 808-0135, Japan*
[b] *Strategic Planning Division, General Coordination Department, Japan Oil, Gas and Metals National Corporation (JOGMEC), 2-10-1 Toranomon, Minato-ku, Tokyo 105-0001, Japan*

ARTICLE INFO

Article history:
Received 26 June 2013
Received in revised form
27 September 2013
Accepted 9 October 2013
Available online 8 November 2013

Keywords:
Near-critical phase
Hybrid catalyst
Syngas to hydrocarbons
Pd/ZSM-5
Gasoline fraction
Methanol to hydrocarbons

ABSTRACT

The conversion of syngas ($CO + H_2$) to hydrocarbons in gasoline fraction over a hybrid catalyst composed of Cu-ZnO and Pd/ZSM-5 in a near-critical *n*-hexane solvent was investigated. Methanol was synthesized from syngas over Cu-ZnO; subsequently, was converted to hydrocarbons through the formation of dimethyl ether (DME) over Pd/ZSM-5. The yield of hydrocarbons increased from ca. 29% to ca. 54% with increasing the partial pressure of *n*-hexane from 0 MPa to 1.5 MPa. By contrast, the yields of CO_2 and DME decreased with increasing the partial pressure of *n*-hexane. A decrease in the particle size of ZSM-5 as well as an increase in a Pd loading led to the selective production of hydrocarbons in the gasoline fraction. The hybrid catalyst containing 0.5 wt% Pd/ZSM-5 with ca. 100 nm in size exhibited 51% gasoline fraction yield with 75% CO conversion. The catalyst stability was also improved by increasing the Pd loading during the reaction.

1. Introduction

Because of a drastic increase in worldwide energy consumption, the development of hydrocarbon production processes with carbon resources alternative to crude oil has been highly desirable. Syngas ($CO + H_2$), which can be produced from a variety of carbon resources such as natural gas, biomass, and coal, has been focused on as a raw material for the production of fuels and chemicals. Syngas can be converted directly to hydrocarbons through the Fischer-Tropsch synthesis (FTS) [1–7]. Another way of uses of syngas is the production of methanol. Methanol can be utilized for the production of hydrocarbons through the methanol-to-hydrocarbons (MTH) reaction using zeolites or zeolite-type catalysts. In the MTH reaction, hydrocarbon distribution is strongly dependent on the micropore size of zeolites, and the production of heavy hydrocarbons such as diesel fraction hydrocarbons are strictly inhibited [8–12]. Thus, a process of the methanol synthesis from syngas following the MTH reaction would be effective on the selective production of light hydrocarbons with the efficient utilization of the alternative carbon resources.

By employing hybrid catalysts composed of a methanol synthesis catalyst, e.g. Pd/SiO_2, Cu-ZnO and Cr-ZnO, and a zeolite catalyst, e.g. ultra-stable Y zeolite (USY) and beta zeolite, the direct synthesis of light hydrocarbons in liquefied petroleum gas (LPG) fraction from syngas has been developed [13–17]. In these LPG synthesis processes, syngas can be primarily converted to methanol over the metal-based catalyst. Subsequent conversion of methanol to hydrocarbons readily takes place over the zeolite which neighbors the metal-based catalyst in the hybrid catalyst. The rapid consumption of methanol gives the methanol synthesis from syngas an advantage over the reverse reaction of methanol to syngas over the metal-based catalysts, leading to higher yield of hydrocarbons than the calculated value based on the thermodynamic equilibrium [13].

ZSM-5, a **MFI**-type aluminosilicate material, is well known as a zeolite catalyst having the pore size and acid properties suitable for the production of gasoline-range hydrocarbons in the MTH reaction [8–10]. Considering the selective production of specified fuel hydrocarbons, the employment of a hybrid catalyst containing ZSM-5 would be suitable for the hydrocarbon production from syngas. Furthermore, since olefins are primarily produced in the MTH reaction, metal catalysts with high hydrogenation ability are required for obtaining paraffins as a final product. It was reported that Pd supported on zeolite efficiently converts olefins to paraffins during the conversion of syngas to hydrocarbons [15]. Thus,

---

[*] Corresponding author. Tel.: +81 93 695 3733; fax: +81 93 695 3398.
E-mail address: h-imai@kitakyu-u.ac.jp (H. Imai).

0920-5861/$ – see front matter © 2013 Elsevier B.V. All rights reserved.
http://dx.doi.org/10.1016/j.cattod.2013.10.037

Pd/ZSM-5 is expected to efficiently produce paraffins in gasoline fraction from methanol that is generated from syngas.

Reaction processes using solid catalysts in near- and supercritical solvents have received considerable attention in the fields of organic synthesis [18–21] and biomass conversion [22–26] in the recent decades because a reaction rate can be significantly improved in the solvents. Supercritical hydrocarbon fluids have been applied to the FTS to increase the hydrocarbon yield and to suppress the generation of undesired products due to the efficient extraction of products from catalysts [27–31]. In a manner similar to the FTS reaction in the supercritical phase, the LPG synthesis from syngas using a hybrid catalyst in a near-critical solvent of *n*-hexane has been studied [32]. Efficient removal of heat generated during the reaction by the near-critical fluid leads to improvements in the stability of the catalyst as well as the selectivity for light hydrocarbons. In this paper, the term "near-critical" is used to connote the region close to the critical temperature and pressure of *n*-hexane.

In this study we investigated the catalytic activity of a hybrid catalyst composed of Cu-ZnO and Pd/ZSM-5 in a near-critical *n*-hexane solvent in the conversion of syngas to hydrocarbons via methanol. During the experimental trials, the reaction in the near-critical phase was compared with those in conventional phases to clarify the effect of the near-critical solvent on the catalytic activity and product distribution. We also investigated the effects of the acid amount and particle size of ZSM-5 as well as Pd loading on the hydrocarbon yield.

2. Experimental

2.1. Catalyst preparation

A hybrid catalyst was prepared by physically mixing the 355–710 μm pellets of a Cu-ZnO methanol synthesis catalyst of 0.5 g with those of a Pd/ZSM-5 catalyst of 0.5 g. Cu-ZnO was a commercial catalyst (MK-121, TOPSØE). Pd/ZSM-5 was prepared by impregnation method with a 4.557 wt% $Pd(NH_3)_2(NO_3)_2$ aqueous solution and commercial ZSM-5 with the SiO_2/Al_2O_3 molar ratio of 23 (CBV2314, Zeolyst) or 80 (CBV8014, Zeolyst). Commercial NH_4^+-type ZSM-5 was calcined at 823 K for 3 h to become proton-type ZSM-5. Proton-type ZSM-5 was immersed in the $Pd(NH_3)_2(NO_3)_2$ aqueous solution with a supported Pd weight at room temperature overnight. The resultant was evaporated at 333 K, dried at 393 K for 3 h, and calcined at 823 K for 3 h. In addition, a **MFI** zeolite was hydrothermally synthesized by using an aluminosilicate gel with the SiO_2/Al_2O_3 ratio of 23 and tetrapropylammonium hydroxide (TPAOH) as a structure-directing agent (SDA) at 443 K for 24 h, according to the previous report [33]. The obtained Na^+-type **MFI** zeolite was transformed to a proton-type **MFI** zeolite by ion-exchange treatment with 2.2 M NH_4NO_3 aqueous solution followed by calcination at 823 K for 3 h.

2.2. Characterization

The structure of the catalysts was examined by X-ray diffraction (XRD, Rigaku XRD-DSC-XII). The diffractometer was operated at 40 kV and 20 mA using Cu-Kα radiation source. XRD patterns were recorded at 6 degree/min over the angular range of 5–50°. The SiO_2/Al_2O_3 ratios of the samples were determined by X-ray fluorescence analysis (XRF, Rigaku ZSX101E). The BET surface area and micropore volume were estimated from nitrogen adsorption isotherms at 77 K with a Micromeritics ASAP 2010 instrument. Prior to the analyses, the sample was treated at 573 K for 3 h under nitrogen flow in order to remove adsorbed compounds. External surface area (S_{EXT}) was estimated by the *t*-plot method. Field-emission scanning electron microscopic (FE-SEM) images of the catalysts were obtained on an S-5200 microscope (Hitachi) operating at 10–15 kV.

Temperature programmed ammonia desorption (NH_3-TPD) profiles were recorded on BELCAT-B (BEL Japan). The sample was pretreated under a He flow at 723 K for 1 h, and then cooled down to 373 K. Ammonia was allowed to make contact with the sample at 373 K for 1 h. Subsequently, the sample was evacuated to remove weakly adsorbed ammonia at 373 K for 30 min. Finally, the sample was heated from 373 K to 883 K at a raising rate of 10 K/min in a He flow. The desorbed ammonia was monitored on a TCD.

Temperature programmed hydrogen desorption (H_2-TPD) profiles were recorded on BELCAT-B (BEL Japan). The sample was pretreated under a He flow at 473 K for 5 h, and then reduced under 10 vol% H_2 balanced by He at 573 K for 10 h. After cooling down to 323 K, a mixed gas composed of 10 vol% H_2 and He balance flowed into the sample for 1 h. Finally, the sample was heated from 323 K to 923 K at raising rate of 10 K/min in a He flow. A mass spectrometer was used to monitor the desorbed hydrogen (m/e = 2).

2.3. Catalytic reaction test

A pressurized flow type of reaction apparatus with a fixed-bed reactor was used for this study. The experimental set-up scheme is shown in Fig. 1. The apparatus was equipped with an electronic temperature controller for a furnace, a vaporizer of a solvent, a stainless tubular reactor with an inner diameter of 6 mm, thermal mass flow controllers for gas flows and a back-pressure regulator. A solvent was pumped into the reactor by a high-pressure pump. 1 g of a hybrid catalyst was loaded in the reactor, and inert glass sand was placed above and below the catalyst. The length of the catalyst bed was about 6.0–6.5 cm. The catalyst was reduced in a flow of a mixture of 5% hydrogen and 95% nitrogen with 100 mL min^{-1} at 573 K for 3 h. After the reduction of the catalyst, the catalyst was cooled down to 473 K. Syngas (60% H_2, 32% CO, 5% CO_2, and 3% Ar) and *n*-hexane as a solvent were introduced into the catalyst to make the total pressure inside reach to 4.0 MPa in a He flow, and then the catalyst was heated up to 553 K. The partial pressure of syngas, P_{syngas}, of 2.5 MPa was retained, and the partial pressure of *n*-hexane, $P_{n\text{-hexane}}$, was varied from 0 MPa to 1.5 MPa. The catalyst weight to the flow rate ratio ($W/F_{\text{-syngas}}$) was 9.7 $g_{\text{-cat}}$ h/$mol_{\text{-syngas}}$. CO, CO_2 and CH_4 of the reaction products were analyzed with an on-line gas chromatograph (Shimadzu GC-8A) equipped with a thermal conductivity detector (TCD) and a packed column of activated charcoal. The light hydrocarbon products were analyzed with another on-line gas chromatograph (Shimadzu GC-2014) equipped

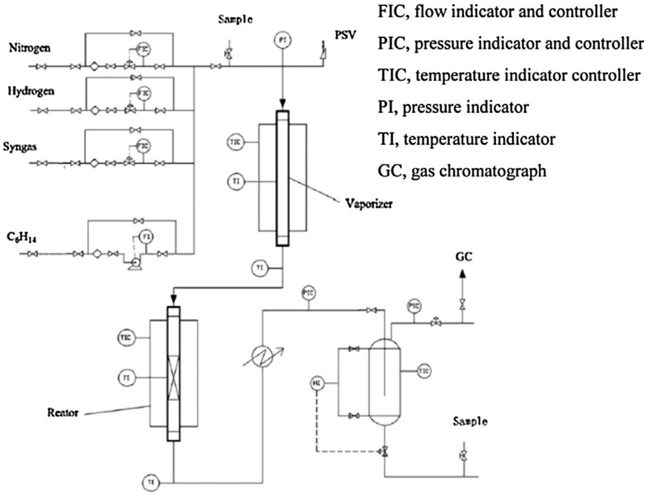

Fig. 1. Scheme of experimental set-up.

with a flame ionization detector (FID) and a capillary column of Porapak-Q. The products liquefied by condensation at room temperature were analyzed with an off-line gas chromatograph (Shimadzu GC-2014) equipped with an FID detector and a capillary column of TC-1. For the analyses of the liquefied products, decahydronaphthalene ($C_{10}H_{18}$) was used as an internal standard.

2.4. Calculation method

The conversion of CO was defined as

$$\text{CO conversion}\,(\%) = \left(1 - \frac{\text{CO}_{\text{out}}\,(\text{mol})}{\text{CO in feed}\,(\text{mol})}\right) \times 100$$

The yield of C-containing products was defined based on the atomic carbon. The yield of CO_2 was defined as

$$\text{CO}_2\text{ yield}\,(\text{C-\%}) = \frac{\text{CO}_2\,(\text{mol})}{\text{CO in feef}\,(\text{mol})} \times 100$$

The yield of DME was defined as

$$\text{DME yield}\,(\text{C-\%}) = \frac{\text{DME}\,(\text{mol}) \times 2}{\text{CO in feed}\,(\text{mol})} \times 100$$

The yield of hydrocarbon was defined as

$$\text{C}_n\ \ \text{yield}\,(\text{C-\%}) = \frac{\text{C}_n\,(\text{mol}) \times n}{\text{CO in feed}\,(\text{mol})} \times 100$$

3. Results and discussion

3.1. Conversion of syngas to hydrocarbons over hybrid catalyst in near-critical phase

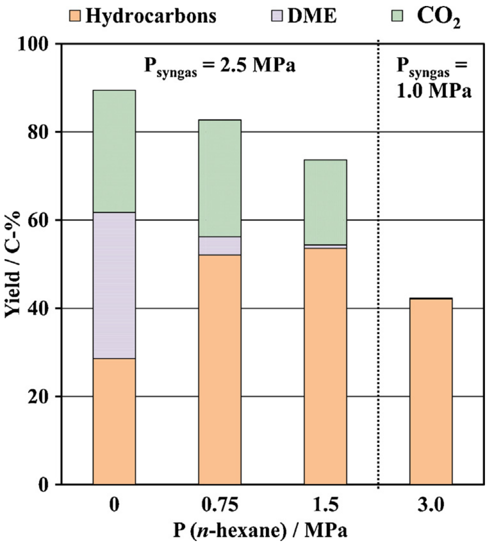

Fig. 2. Product yield resulting from conversion of syngas to hydrocarbons over hybrid catalyst composed of Cu-ZnO and 0.5 wt% Pd/ZSM-5 as a function of partial pressure of *n*-hexane. *Reaction conditions*: cat., 1.0 g hybrid catalyst (0.5 g Cu-ZnO and 0.5 g Pd/ZSM-5); temp., 553 K; P_{total} = 4.0 MPa (balanced by He); P_{syngas} = 2.5 MPa or 1.0 MPa; W/F = 9.7 $g_{\text{-cat}}$ h/$mol_{\text{-syngas}}$; H_2/CO = 1.9.

The catalytic activity of a hybrid catalyst composed of Cu-ZnO and Pd/ZSM-5 in a near-critical *n*-hexane solvent was investigated in the conversion of syngas to hydrocarbons via methanol. 0.5 wt% Pd was supported on ZSM-5 with the SiO_2/Al_2O_3 ratio of 23. Fig. 2 shows product yields resulting from the syngas conversion over the hybrid catalyst. The partial pressure of *n*-hexane was varied from 0 MPa to 1.5 MPa with the syngas partial pressure of 2.5 MPa constant. The critical pressure and critical temperature of *n*-hexane are 507.5 K and 3.01 MPa, respectively. The total pressure in the reaction system of 4.0 MPa was kept with He as a carrier gas during the reaction. CO conversion decreased from ca. 90% to ca. 74% as the partial pressure of *n*-hexane increased from 0 to 1.5 MPa. The employment of supercritical fluids resulted in decreasing CO conversion in the FT synthesis due to lower diffusion efficiency of syngas compared with that in gas phase [13,30,34]. It is indicated that the near-critical fluid also suppressed the diffusion of syngas during the reaction to decrease the CO conversion in this study. Hydrocarbon yield was drastically increased by co-feeding *n*-hexane with syngas to the catalyst, and increased from ca. 29% to ca. 54% with the increase in the partial pressure of *n*-hexane from 0 to 1.5 MPa. Hydrocarbon distributions at 6.5 h after the reaction started are shown in Fig. 3. By employing the near-critical fluid ($P_{n\text{-hexane}}$ = 1.5 MPa), hydrocarbons with carbon numbers of 5–9 were efficiently produced, while the selectivities of ethane and propane decreased. In contrast to the hydrocarbon yield, DME yield was decreased from 33% to 0.8% by the employment of the near-critical solvent. In order to compare the catalytic properties of the hybrid catalyst in the near-critical fluid with those in a supercritical fluid, the partial pressure of *n*-hexane was increased to 3.0 MPa, while the partial pressure of syngas was decreased to 1.0 MPa to keep the total pressure at 4.0 MPa. Surprisingly, DME and CO_2 were little detected, and hydrocarbons were dominantly produced although the CO conversion decreased due to the decrease in the partial pressure of syngas. The employment of *n*-hexane as the near-critical solvent improves the heat transfer during the reaction, leading to the increase in the LPG yield through the conversion of methanol [32]. It is suggested that the introduction of *n*-hexane as the near-critical solvent improved the conversion of DME to hydrocarbons due to the good heat transfer in the near-critical phase.

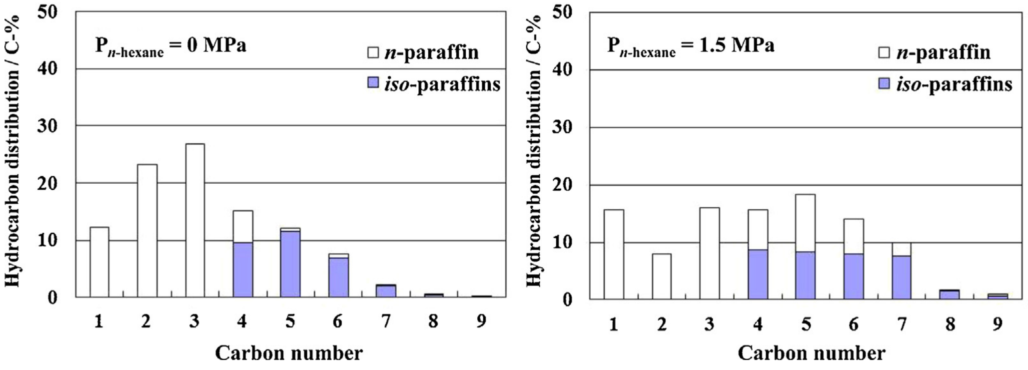

Fig. 3. Hydrocarbon distributions resulting from conversion of syngas to hydrocarbons over hybrid catalyst composed of Cu-ZnO and 0.5 wt% Pd/ZSM-5. *Reaction conditions*: cat., 1.0 g hybrid catalyst (0.5 g Cu-ZnO and 0.5 g Pd/ZSM-5); temp., 553 K; P_{total} = 4.0 MPa (balanced by He); P_{syngas} = 2.5 MPa; W/F = 9.7 $g_{\text{-cat}}$ h/$mol_{\text{-syngas}}$; H_2/CO = 1.9.

The yield of CO_2 decreased with increasing the partial pressure of *n*-hexane. CO_2 is generated through the water-gas shift (WGS) reaction of CO with H_2O over Cu-ZnO. Supercritical fluids in the FT processes extracts H_2O generated during the reaction from the catalyst, while the extraction capability of the fluids to H_2O is proportional to the partial pressure of the fluids due to low affinity of H_2O to organic solvents [29,35]. It is thus suggested that the near-critical fluid helped the emission of H_2O from the surfaces of the catalyst, leading to the suppression of the WGS reaction over Cu-ZnO. Considering the use of high-pressure equipment (supercritical system), it generally costs much to set up apparatuses which can be safely operated under sever conditions. Thus, processes with the near-critical *n*-hexane fluid are expected to be economical due to easier handling of apparatuses for the selective production of gasoline-range hydrocarbons from syngas via methanol using hybrid catalysts.

3.2. Effect of acid amount of ZSM-5 on catalytic activity

Product distribution in the MTH reaction is strongly dependent on physicochemical properties of zeolites including acid amount, pore size and crystal size. In order to investigate the effect of the acid amount of ZSM-5 in the hybrid catalyst on the catalytic properties, the syngas conversion to hydrocarbons was conducted over hybrid catalysts containing ZSM-5 with different SiO_2/Al_2O_3 ratios. The results obtained in the reaction are shown in Fig. 4. The CO conversion increased with increasing the Al content of ZSM-5. In addition, the increase in the Al content of ZSM-5 increased the yield of the hydrocarbons, while the yield of DME drastically decreased. The trends resulting from the reaction are consistent with those obtained using beta zeolite in the LPG synthesis [32]. Fig. 5 shows NH_3-TPD profiles of the 0.5 wt% Pd/ZSM-5 catalysts. The peaks which appeared at higher temperature (573–873 K) correspond to NH_3 desorption from catalytically active acid sites [36,37]. The acid amount of ZSM-5 was strongly dependent on the Al content of ZSM-5, and the acid amounts estimated from the NH_3-TPD profiles were 0.67 mmol g^{-1} and 0.26 mmol g^{-1} for 0.5 wt% Pd/ZSM-5 with the SiO_2/Al_2O_3 ratio of 23 and that with the SiO_2/Al_2O_3 ratio of 80, respectively. The conversion of methanol or DME to hydrocarbons should depend on the amount of acid sites of zeolite catalysts. The large amount of the acid sites is probably required for the complete conversion of methanol to hydrocarbons via DME at low temperature below 573 K, compared with the MTH reaction carried out at temperatures of 623–723 K. Therefore, ZSM-5 with the higher Al content was advantageous to yielding hydrocarbons from syngas via methanol or DME.

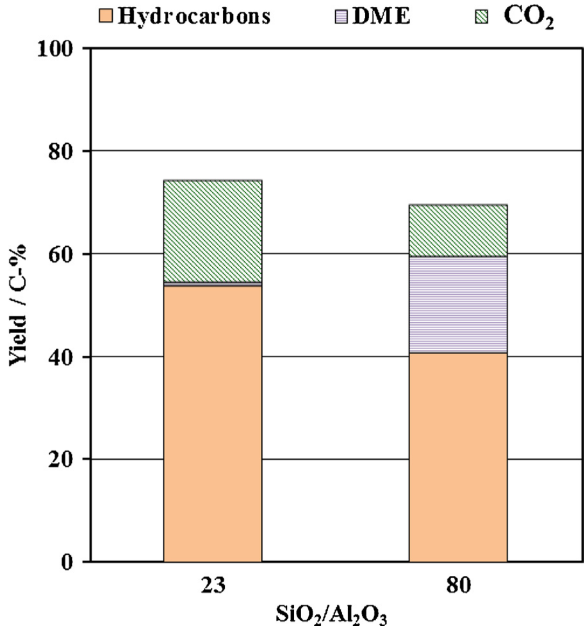

Fig. 4. Product yield resulting from conversion of syngas to hydrocarbons over hybrid catalysts composed of Cu-ZnO and 0.5 wt% Pd/ZSM-5 with different SiO_2/Al_2O_3 ratios. *Reaction conditions*: cat., 1.0 g hybrid catalyst (0.5 g Cu-ZnO and 0.5 g Pd/ZSM-5); temp., 553 K; P_{syngas} = 2.5 MPa; $P_{n\text{-hexane}}$ = 1.5 MPa; W/F = 9.7 $g_{\text{-cat}}$ h/$mol_{\text{-syngas}}$; H_2/CO = 1.9.

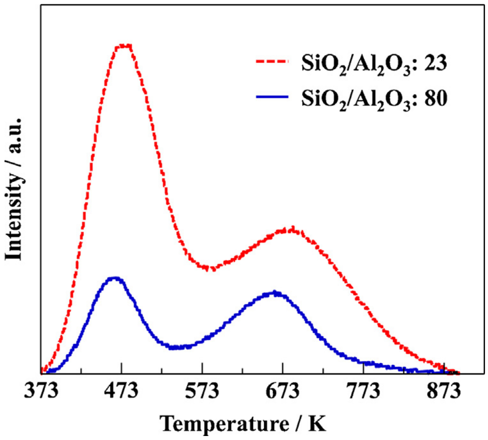

Fig. 5. NH_3-TPD profiles of 0.5 wt% Pd/ZSM-5 samples with different SiO_2/Al_2O_3 ratios.

The generation of CO_2 was mitigated during the reaction when the Al content of ZSM-5 in the hybrid catalyst decreased (Fig. 4). The smaller amount of H_2O could be generated over ZSM-5 with the SiO_2/Al_2O_3 ratio of 80 than over ZSM-5 with the SiO_2/Al_2O_3 ratio of 23 due to the insufficient conversion of DME to hydrocarbons, resulting in the suppression of the CO_2 generation through the WGS reaction.

3.3. Effect of particle size of ZSM-5 on catalytic activity

The effect of the particle size of Pd/ZSM-5 on the catalytic activity was investigated using ZSM-5 with different particle sizes. Fig. 6 shows XRD patterns and SEM images of commercial ZSM-5 (CBV2314, Zeolyst) and hydrothermally synthesized ZSM-5 using tetraorthosilicate as a silica source and TPAOH as an SDA. Both samples exhibited the typical patterns assigned to the **MFI** structure (Fig. 6A). The FE-SEM images revealed that commercial ZSM-5 (ZSM-5-CM) was composed of cuboid blocks with an average size of ca. 600 nm, while hydrothermally synthesized ZSM-5 (ZSM-5-HT) was composed of cubic crystallites about 100 nm in size (Fig. 6B). The physicochemical properties of both the ZSM-5 samples are summarized in Table 1. The SiO_2/Al_2O_3 ratio of 32 for ZSM-5-HT was similar to that of 23 for ZSM-5-CM. The surface area (S_{BET}) of ZSM-5-HT (373 $m^2 g^{-1}$) was also close to that of ZSM-5-CM (363 $m^2 g^{-1}$). By contrast, the external surface area (S_{EXT}) of ZSM-5 increased due to a decrease in the particle size.

Fig. 7 shows the product yields of ZSM-5-CM and ZSM-5-HT in the syngas conversion to hydrocarbons via methanol. The CO conversion was independent of the particle size of the ZSM-5 sample. In addition, the yields of CO_2, DME and the hydrocarbons generated over the hybrid catalyst containing ZSM-5-CM were very similar to those of the hybrid catalyst containing ZSM-5-HT. These results indicate that the particle size of the zeolite influences little the catalytic activity of the zeolite for the methanol conversion to hydrocarbons. By contrast, the product distribution, especially the hydrocarbon distribution, was strongly dependent on the particle size of ZSM-5. Fig. 8 shows hydrocarbon distributions over

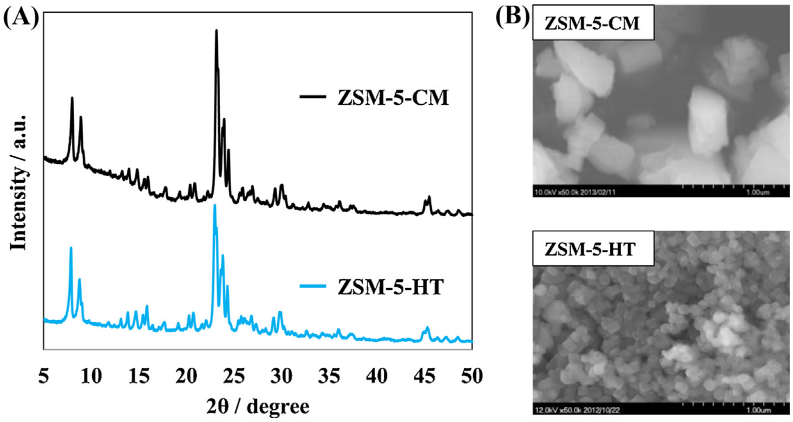

Fig. 6. XRD patterns (A) and SEM images (B) of commercial ZSM-5 (CBV2314) (ZSM-5-CM) and hydrothermally synthesized ZSM-5 (ZSM-5-HT).

Table 1
Physicochemical properties of commercial and hydrothermal synthesized ZSM-5 catalysts.

Sample	SiO_2/Al_2O_3 [a]	Size[b] (nm)	S_{BET} [c] ($m^2\ g^{-1}$)	S_{EXT} [d] ($m^2\ g^{-1}$)	V_{micro} [e] ($cm^3\ g^{-1}$)
ZSM-5-CM	23	600	363	54	0.13
ZSM-5-HT	32	100	373	115	0.11
ZSM-5-CM	80	–	440	183	0.13

[a] Estimated from XRF measurement.
[b] Average particle size estimated from FE-SEM observations.
[c] S_{BET}, surface area estimated by N_2 adsorption method.
[d] S_{EXT}, external surface area estimated by N_2 adsorption method.
[e] V_{micro}, micropore volume estimated by N_2 adsorption method.

the hybrid catalysts with ZSM-5-CM or ZSM-5-HT at 6.5 h of the reaction time. The selectivity of hydrocarbon fractions (C_5–C_9) associated with gasoline increased from 44% to 65% with decreasing the particle size of ZSM-5, while those of methan, ethane and propane decreased with decreasing the particle size. In the MTH reaction, the crystal size of zeolites does not significantly influence the selectivity of various hydrocarbon products. However, a decrease in the crystal size retards the deposition of carbonaceous species in the pores and cavities of zeolites due to the high mass transfer of reactants as well as products, leading to the improvement of the catalyst life [33]. On the other hand, it was reported that the carbonaceous species formed in the cavities of the zeolite induced an effect of transition-state shape selectivity due to the reduction of the pore and cavity spaces, promoting the formation of smaller olefins [38,39]. ZSM-5-HT composed of smaller particles than those of ZSM-5-CM exhibited the selective production of the hydrocarbons in the gasoline fraction. In ZSM-5-HT, hydrocarbons generated in the pores of the zeolite could more readily transfer out of the pores during the reaction due to the shorter pore channels in comparison with ZSM-5-CM. It is assumed that the further oligomeration of the products in the pores could be suppressed in ZSM-5-HT, resulting in keeping large cavity spaces. Thus, the efficient transfer of larger hydrocarbons than the LPG and dry gas fractions to out of the pores could take place in ZSM-5-HT. On the other hand, in the cavities of ZSM-5-CM, the transfer of the large hydrocarbons was suppressed by the carbonaceous species deposited, promoting the formation of the small hydrocarbons through the cracking of the large hydrocarbons.

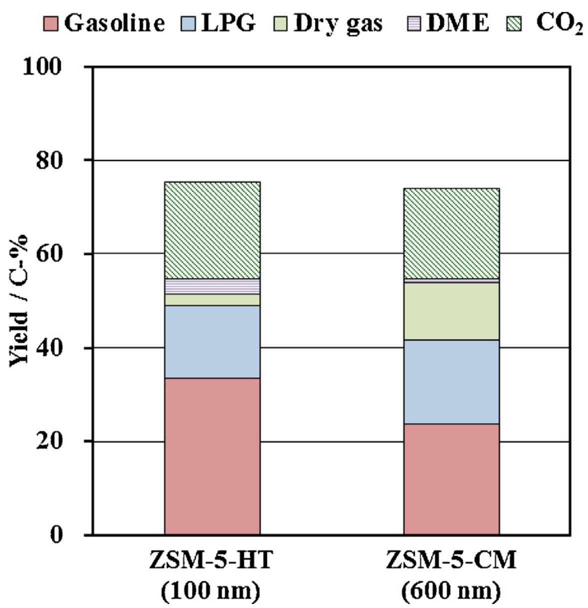

Fig. 7. Product yield resulting from conversion of syngas to hydrocarbons over hybrid catalysts composed of Cu-ZnO and 0.5 wt% Pd/ZSM-5 with different particle sizes. *Reaction conditions*: cat., 1.0 g hybrid catalyst (0.5 g Cu-ZnO and 0.5 g Pd/ZSM-5); temp., 553 K; P_{syngas} = 2.5 MPa; $P_{n\text{-hexane}}$ = 1.5 MPa; W/F = 9.7 $g_{\text{-cat}}$ h/$mol_{\text{-syngas}}$; H_2/CO = 1.9.

3.4. *Effect of mixing way of Cu-ZnO with Pd/ZSM-5 on catalytic properties*

In order to investigate the effects of the catalyst preparation method on the catalytic properties, the hybrid catalysts were prepared by two different methods: powder mixing and granule mixing. In the powder mixing, after Cu-ZnO of 0.5 g and Pd/ZSM-5 of 0.5 g were physically mixed with a mortar, the mixed powder was pelletized, crushed, and then sieved to particles with 355–710 μm. In order to distinguish the physical mixing method of each pelletized particle of Cu-ZnO and Pd/ZSM-5 described in the experimental section from the powder mixing, the usual preparation method is denoted as granule mixing in Fig. 9. The hybrid catalyst prepared by the granule mixing exhibited a slightly higher CO conversion, higher CO_2 yield and lower DME yield than that

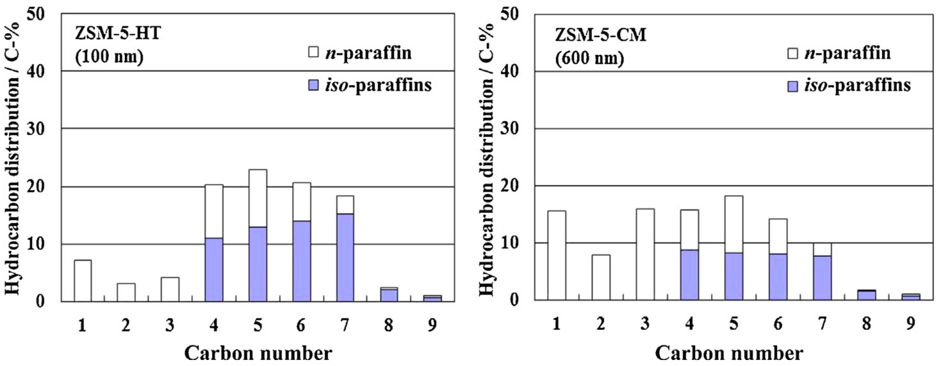

Fig. 8. Hydrocarbon distributions resulting from conversion of syngas to hydrocarbons over hybrid catalyst composed of Cu-ZnO and 0.5 wt% Pd/ZSM-5 with different particle sizes. *Reaction conditions*: cat., 1.0 g hybrid catalyst (0.5 g Cu-ZnO and 0.5 g Pd/ZSM-5); temp., 553 K; P_{syngas} = 2.5 MPa; $P_{n\text{-hexane}}$ = 1.5 MPa; W/F = 9.7 $g_{\text{-cat}}$ h/$mol_{\text{-syngas}}$; H_2/CO = 1.9.

prepared by the powder mixing in the conversion of syngas to hydrocarbons in the near-critical *n*-hexane fluid (Fig. 9). In addition, the catalyst prepared by the granule mixing gave the higher yield (ca. 33%) of gasoline fraction hydrocarbons (C_5–C_9) than the catalyst prepared by the powder mixing. On the catalyst prepared by the powder mixing, hydrogen dissociated on Cu-ZnO could readily transfer to the neighboring Pd/ZSM-5, resulting in the formation of CH_4 through the hydrogenation of CO and CO_2 on the Pd particles. Yoshie et al. reported that a hybrid catalyst prepared by the granule mixing showed a high selectivity and activity in the hydrocarbon synthesis from CO_2 [40].

3.5. Effect of palladium loading on ZSM-5 on catalytic properties

Pd on the zeolite plays roles in the efficient hydrogenation of olefins to paraffins in the syngas conversion to hydrocarbons [15]. Since olefins are primarily produced in the methanol conversion to hydrocarbons, Pd is required for the synthesis of saturated hydrocarbons through the hydrogenation. Fig. 10 shows H_2-TPD profiles of the 0.3 and 0.5 wt% Pd/ZSM-5 samples and the ZSM-5 sample. The adsorption of H_2 on ZSM-5 was almost negligible as a result of the observation of no peak derived from desorbed H_2 molecules. By contrast, on the Pd/ZSM-5 samples, a broadened peak was observed in the range from 673 K to 773 K, indicating that H_2 molecules were adsorbed on only the Pd sites. The amount of the adsorbed H_2 was estimated from the profiles to be 0.017 mmol g^{-1} for 0.3 wt% Pd/ZSM-5 and 0.018 mmol g^{-1} for 0.5 wt% Pd/ZSM-5, respectively. Thus, ZSM-5 with the increased Pd loading is capable of preventing the oligomerization of coke precursors through the hydrogenation of the coke precursors to paraffins.

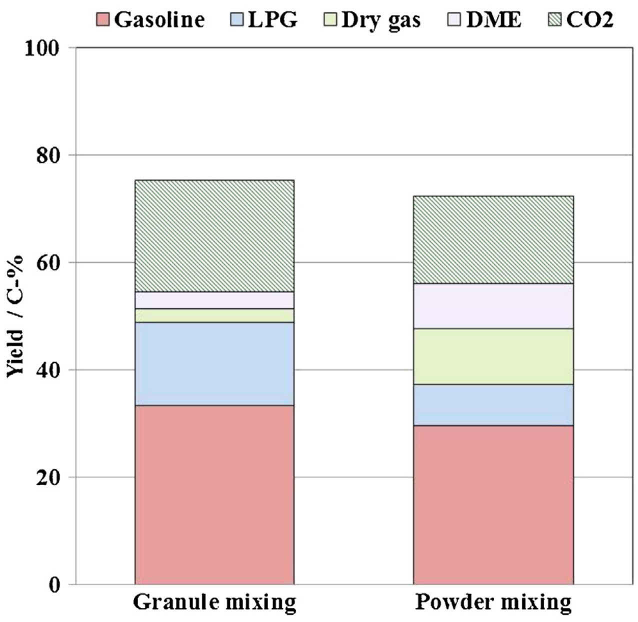

Fig. 9. Influence of mixing way of Cu-ZnO with Pd/ZSM-5 on conversion of syngas to hydrocarbons in near-critical phase over hybrid catalysts composed of Cu-ZnO and 0.5 wt% Pd/ZSM-5. *Reaction conditions*: cat., 1.0 g hybrid catalyst (0.5 g Cu-ZnO and 0.5 g Pd/ZSM-5,); temp., 553 K; P_{syngas} = 2.5 MPa; $P_{n\text{-hexane}}$ = 1.5 MPa; W/F = 9.7 $g_{\text{-cat}}$ h/$mol_{\text{-syngas}}$; H_2/CO = 1.9.

In order to clarify the effects of Pd on the catalytic activity in the syngas conversion, the reaction was carried out employing various Pd loadings on ZSM-5 prepared by the hydrothermal treatment in the hybrid catalyst. The results are shown in Figs. 11 and 12. The hybrid catalyst containing ZSM-5 exhibited 82% CO conversion at 0.5 h after the reaction started. The CO conversion gradually decreased after the reaction started until the conversion reached to ca. 65% at 4 h of the reaction time. By employing the hybrid catalyst composed of Cu-ZnO and Pd supported on ZSM-5, the deactivation became slow, although the initial CO conversion was almost the same (ca. 80%) regardless of the Pd loadings (Fig. 11). The effect of the Pd loadings on the CO conversion was consistent with that obtained in the LPG synthesis over hybrid catalysts composed of Cu-ZnO and Pd/beta [16]. In addition, the hybrid catalysts containing Pd/ZSM-5 exhibited the higher CO conversion at 6.5 h than that with ZSM-5, while the CO conversion at 6.5 h of 0.3 wt% Pd/ZSM-5

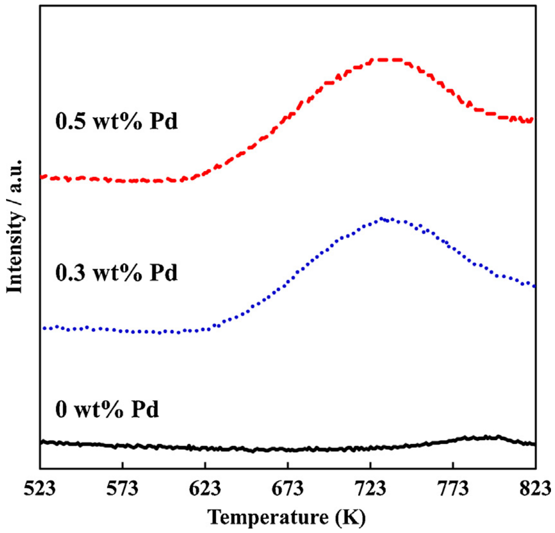

Fig. 10. H_2-TPD profiles of Pd/ZSM-5-HT samples with different Pd loadings.

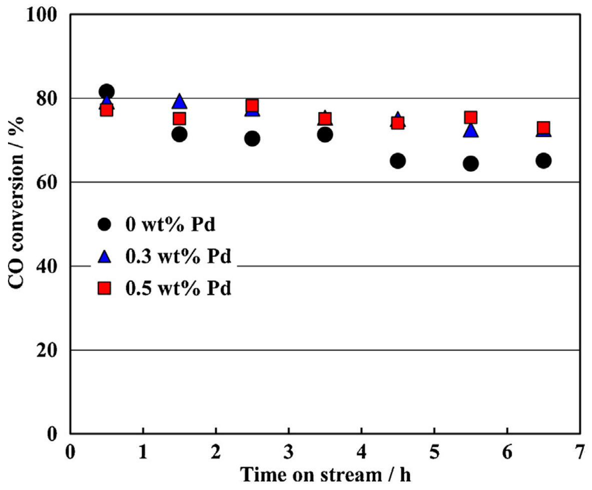

Fig. 11. CO conversion over hybrid catalysts composed of Cu-ZnO and Pd/ZSM-5-HT with different Pd loadings. *Reaction conditions*: cat., 1.0 g hybrid catalyst (0.5 g Cu-ZnO and 0.5 g Pd/ZSM-5); temp., 553 K; P_{syngas} = 2.5 MPa; $P_{n\text{-hexane}}$ = 1.5 MPa; W/F = 9.7 $g_{\text{-cat}}$ h/$mol_{\text{-syngas}}$; H_2/CO = 1.9.

was similar to that of 0.5 wt% Pd/ZSM-5. In the MTH reaction, rapid deactivation occurs due to the deposition of carbonaceous species resulting from the oligomerization of primarily formed unsaturated products on the surface or inside pores of the zeolite [41]. The hydrogenation of the unsaturated products to saturated hydrocarbons over Pd/ZSM-5 would retard the oligomerization to suppress the deactivation.

Fig. 12 shows the product yields of the hybrid catalysts containing ZSM-5, 0.3 wt% Pd/ZSM-5 and 0.5 wt% Pd/ZSM-5. The yield of the hydrocarbons (gasoline, LPG and dry gas) was increased by employing Pd/ZSM-5 as a component of the hybrid catalyst. Moreover, the yield of the hydrocarbons in the gasoline fraction increased from 25% to 33% with the increase in the Pd loadings from 0 wt% to 0.5 wt%, while the yield of the dry gas fractions decreased with increasing the Pd loadings. The increase in the Pd loadings would improve the mass transfer of the products during the reaction because the hydrogenation over Pd leads to suppressing the blocking of the pores and cavities of the zeolite by the carbonaceous species. Therefore, the transfer of the gasoline fractions out of the zeolite intracrystallites was promoted with increasing the Pd loadings; simultaneously, the hydrocracking of the products to small fractions was suppressed. The decrease in the yield of the dry gas fractions with increasing the Pd loading also indicates that the direct hydrogenation of CO to methane was not accelerated even when Pd was employed as a hydrogenation catalyst. In addition, the CO_2 yield was almost the same regardless of the Pd loadings, although the larger amount of H_2O was generated over Pd/ZSM-5 compared with ZSM-5 alone as a result of the methanol conversion to hydrocarbons. These results indicate that Pd hardly contributed to the WGS reaction during the syngas conversion to hydrocarbons.

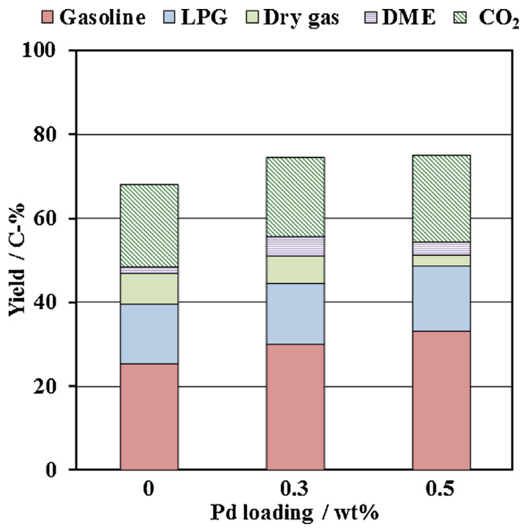

Fig. 12. Product yield resulting from conversion of syngas to hydrocarbons over hybrid catalysts composed of Cu-ZnO and Pd/ZSM-5-HT with different Pd loadings. *Reaction conditions*: cat., 1.0 g hybrid catalyst (0.5 g Cu-ZnO and 0.5 g Pd/ZSM-5); temp., 553 K; P_{syngas} = 2.5 MPa; $P_{n\text{-hexane}}$ = 1.5 MPa; W/F = 9.7 $g_{\text{-cat}}$ h/$mol_{\text{-syngas}}$; H_2/CO = 1.9.

3.6. Catalytic stability of hybrid catalyst in near-critical and gas phases

As shown in Fig. 13, in the conversion of syngas to hydrocarbons in the near-critical phase of *n*-hexane, the hybrid catalyst consisting of Cu-ZnO and 0.5 wt% Pd/ZSM-5 exhibited the higher CO conversion with the lower selectivity of CO_2 in comparison with the reaction in the gas phase under the conditions at 553 K and 4.0 MPa.

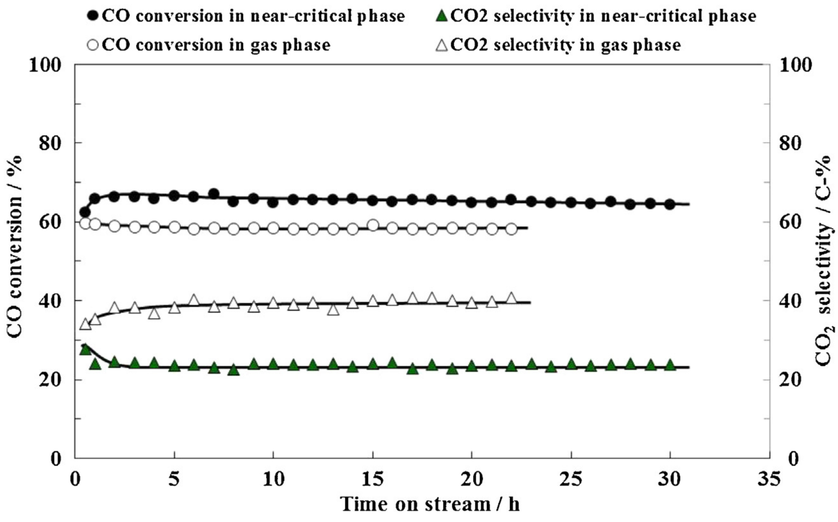

Fig. 13. Conversion of syngas to hydrocarbons over the hybrid catalyst consisting of Cu-ZnO and 0.5 wt% Pd/ZSM-5. *Reaction conditions*: cat., 1.0 g hybrid catalyst (0.5 g Cu-ZnO and 0.5 g Pd/ZSM-5); temp., 553 K; W/F = 9.7 $g_{\text{-cat}}$ h/$mol_{\text{-syngas}}$; H_2/CO = 1.9; P_{syngas}/$P_{n\text{-hexane}}$ = 2.5 MPa/0 MPa (gas phase); P_{syngas}/$P_{n\text{-hexane}}$ = 2.5 MPa/1.5 MPa (near-critical phase).

The CO conversion of ca. 65% was kept until 30 h of the reaction in the near-critical phase. Similar to the reaction in the near-critical phase, in the gas phase, the CO conversion was kept with a constant value of 58% during the reaction although the CO_2 selectivity slightly increased at the initial stage of the reaction.

The deactivation of the catalyst can be mitigated through better heat and mass transfer, leading to prolonging the longevity of catalyst. Owing to the advantages mentioned above, the reaction system with a hybrid catalyst consisting of Cu-ZnO and Pd/ZSM-5 in a near-critical phase is promising for commercial application of the synthesis of gasoline fraction hydrocarbons from syngas.

4. Conclusions

The catalytic performances of hybrid catalysts composed of Cu-ZnO and Pd/ZSM-5 in the syngas conversion to hydrocarbons via methanol in a near-critical *n*-hexane solvent have been studied. The near-critical fluid was effective in the selective production of hydrocarbons in gasoline fraction during the syngas conversion over the hybrid catalyst. In addition, the employment of the near-critical solvent led to depressing the formation of CO_2 during the reaction.

The characteristics of Pd/ZSM-5 influenced the synthesis of the hydrocarbons in the syngas conversion. An increase in the acid amount of ZSM-5 was effective on the generation of hydrocarbons in the syngas conversion to hydrocarbons at lower temperature than those applied in the MTH reaction. Hydrocarbon distribution was strongly dependent on the particle size of ZSM-5 and Pd loading. A decrease in the particle size of ZSM-5 and an increase in the Pd loading improved the yield of hydrocarbons in gasoline fraction with high catalytic stability. It is likely that the improvement of the mass transfer due to the decrease of the particle size and the hydrogenation of unsaturated hydrocarbons over Pd suppress the deposition of carbonaceous species. Subsequently, the pore and cavity spaces in the zeolite can be retained, leading to the smooth mass transfer of large hydrocarbons out of the intracrystallites. Therefore, Pd/ZSM-5 composed of nano-sized particles is effective on the selective production of gasoline fractions from syngas via methanol with the near-critical fluid.

References

[1] R.B. Anderson, Fischer–Tropsch Synthesis, Academic Press, New York, 1984.
[2] M.E. Dry, Appl. Catal. A: Gen. 276 (2004) 1–3.
[3] B.H. Davis, Ind. Eng. Chem. Res. 46 (2007) 8938–8945.
[4] H. Schulz, in: B.H. Davis, M.L. Occelli (Eds.), Fischer–Tropsch Synthesis and Hydroformylation on Cobalt Catalysts, CRC Press/Taylor and Francis Group, Boca Raton/London/New York, 2010, pp. 165–183.
[5] L. Shi, Y. Jin, C. Xing, C. Zeng, T. Kawabata, K. Imai, K. Matsuda, Y. Tan, N. Tsubaki, Appl. Catal. A: Gen. 435-436 (2012) 217–224.
[6] B. Todic, T. Bhatelia, G.F. Froment, W. Ma, G. Jacobs, B.H. Davis, D.B. Bukur, Ind. Eng. Chem. Res. 52 (2013) 669–679.
[7] N.E. Tsakoumis, R. Dehghan, R.E. Johnsen, A. Voronov, W. van Beek, J.C. Walmsley, Ø. Borg, E. Rytter, D. Chen, M. Rønning, A. Holmen, Catal. Today 205 (2013) 86–93.
[8] M. Stöcker, Microporous Mesoporous Mater. 29 (1999) 3–48.
[9] M. Stöcker, Microporous Mesoporous Mater. 82 (2005) 257–292.
[10] T. Mokrani, M. Scurrell, Catal. Rev. 51 (2009) 1–145.
[11] B. Vora, J.Q. Chen, A. Bozzano, B. Glover, P. Barger, Catal. Today 141 (2009) 77–83.
[12] J.F. Haw, W. Song, D.M. Marcus, J.B. Nicholas, Acc. Chem. Res. 36 (2003) 317–326.
[13] Q. Zhang, X. Li, K. Asami, S. Asaoka, K. Fujimoto, Fuel Process. Technol. 85 (2004) 1139–1150.
[14] K. Asami, Q. Zhang, X. Li, S. Asaoka, K. Fujimoto, Catal. Today 106 (2005) 247–251.
[15] Q. Ge, X. Li, H. Kaneko, K. Fujimoto, J. Mol. Catal. A 278 (2007) 215–219.
[16] Q. Ge, Y. Lian, X. Yuan, X. Li, K. Fujimoto, Catal. Commun. 9 (2008) 256–261.
[17] X. Ma, Q. Ge, J. Ma, H. Xu, Fuel Process. Technol. 109 (2013) 1–6.
[18] M.G. Hiltzler, M. Poliakoff, Chem. Commun. (1997) 1667–1668.
[19] A. Baiker, Chem. Rev. 99 (1999) 453–473.
[20] P.G. Jessop, W. Leitner (Eds.), Chemical Synthesis Using Supercritical Fluids, Wiley, New York, 1999.
[21] C.V. Rode, U.D. Joshi, O. Sato, M. Shirai, Chem. Commun. 9 (2003) 1960–1961.
[22] Y. Matsumura, T. Minowa, B. Potic, S.R.A. Kersten, W. Prins, W.P.M. van Swaaij, B. van de Beld, D.C. Elliott, G.G. Neuenschwander, A. Kruse, M.J. Antal Jr., Biomass Bioenergy 29 (2005) 269–292.
[23] A.A. Peterson, F. Vogel, R.P. Lachance, M. Fröling, M.J. Antal Jr., J.W. Tester, Energy Environ. Sci. 1 (2008) 32–65.
[24] D.C. Elliott, Biofuels Bioprod. Biorefining 2 (2008) 254–265.
[25] A. Yamaguchi, N. Hiyoshi, O. Sato, M. Shirai, Green Chem. 13 (2011) 873–881.
[26] E. Markočič, B. Kramberger, J.G. Van Bennekom, H. Jan Heeres, J. Vos, Ž. Knez, Renew. Sustain. Energy Rev. 23 (2013) 40–48.
[27] N. Tsubaki, K. Yoshii, K. Fujimoto, J. Catal. 207 (2002) 371–375.
[28] W. Linghu, X. Li, K. Asami, K. Fujimoto, Fuel Process. Technol. 85 (2004) 1121–1138.
[29] R.M. Malek Abbaslou, J.S. Soltan Mohammadzadeh, A.K. Dalai, Fuel Process. Technol. 90 (2009) 849–856.
[30] A.K. Mogalicherla, N.O. Elbashir, Energy Fuels 25 (2011) 878–889.
[31] E.E. Elmalik, E. Tora, M. El-Halwagi, N.O. Elbashir, Fuel Process. Technol. 92 (2011) 1525–1530.
[32] Q. Zhang, P. Liu, Y. Fujiyama, C. Chen, X.H. Li, Appl. Catal. A: Gen. 401 (2011) 147–152.
[33] H. Mochizuki, T. Yokoi, H. Imai, R. Watanabe, S. Namba, J.N. Kondo, T. Tatsumi, Microporous Mesoporous Mater. 145 (2011) 165–171.
[34] A.K. Mogalicherla, E.E. Elmalik, N.O. Elbashir, Chem. Eng. Process.: Process Intensification 62 (2012) 59–68.
[35] K. Yokota, Y. Hanaoka, K. Fujimoto, Fuel 70 (1991) 989–994.
[36] M. Niwa, N. Katada, Catal. Surv. Jpn. 1 (1997) 215–226.
[37] K. Suzuki, Y. Aoyagi, N. Katada, M. Choi, R. Ryoo, M. Niwa, Catal. Today 132 (2008) 38–45.
[38] D. Chen, K. Moljord, T. Fuglerud, A. Holmen, Microporous Mesoporous Mater. 29 (1999) 191–203.
[39] D. Chen, K. Moljord, A. Holmen, Microporous Mesoporous Mater. 164 (2012) 239–250.
[40] S. Yoshie, F. Masahiro, K. Roger, A. Hisanori, Q. Xu, Stud. Surf. Sci. Catal. 114 (1998) 327–332.
[41] H. Schulz, Catal. Today 154 (2010) 183–194.